Colloid & Polymer Science Colloid Polym Sci 272:1403–1419 (1994)

Short-range order effects in amorphous polycondensates as studied by spin polarized diffuse neutron scattering and simulation*)

C. Lamers[1]), C. Schönfeld[1]), S. M. Shapiro[4]), J. Batoulis[2]), R. Timmermann[2]), J. W. Cable[3]), and D. Richter[1])

[1]) Institut für Festkörperforschung, Forschungszentrum Jülich, FRG
[2]) Bayer AG, Leverkusen, FRG
[3]) Oak Ridge National Laboratory, Oak Ridge, Tennessee, USA
[4]) Brookhaven National Laboratory, Upton, New York, USA

*) *Dedicated to Professor Dr. E. W. Fischer on the occasion of his 65th birthday.*

Abstract: Short-range order effects in amorphous polycondensates, including the technologically important bisphenol-A-polycarbonate, have been investigated by elastic diffuse neutron scattering with spin polarization analysis. Selectively deuterated samples of each polycondensate have been used in order to vary the scattering contrast and thereby emphasize different pair correlations. The technique of spin polarization analysis allowed a reliable separation of the coherent scattering and an intensity calibration on the basis of the incoherent scattering as an internal standard. Thus, $(d\sigma/d\Omega)_{coh}$ has been measured directly by this method. The experimental results are compared to calculated cross-sections from computer-generated structures. Simulations have been performed with the "amorphous cell" method which models the static structure of the amorphous polymer in full chemical detail on the basis of a "random coil" conformation. The results of the simulations yield a fertile ground for the discussion of the measured cross-sections, though a direct comparison with the experiment is not always satisfactory. The observed discrepancies indicate a still insufficient structural relaxation of the simulated structures.

Key words: Polycarbonate – partial structure factors – neutron scattering – simulation

Introduction

The polymer glass bisphenol-A-polycarbonate (BPA-PC), i.e., the polycarbonate of 2,2-bis(4-hydroxyphenyl) propane, has found a wide range of applications for consumer products because of its high impact strength and temperature resistance. Due to its technological importance, numerous x-ray and neutron scattering studies have been performed to investigate the static structure and especially the short range order in BPA-PC and related polycarbonates [1–13]. The dynamics in BPA-PC, which are essential for the understanding of the high energy dissipation even at low temperatures, were studied by NMR [14–18], dynamic-mechanical relaxation [19–21] and, most recently, by quasielastic neutron scattering [22]. In the first scattering experiments on polycarbonates the structure of crystalline BPA-PC was determined by x-ray crystallography [1, 3], where an orthorhombic or monoclinic unit cell was found containing four chains with two monomers each in a zig-zag configuration. For non-crystalline polycarbonate, a "nodular" conformation containing crystalline-like ordered regions with diameters of 60 to 100 Å was proposed on the basis of electron microscopic investigations [23–28]. However, by careful analysis of

scattering experiments with x-rays and neutrons [29–31] this "nodule" hypothesis was proven to be incorrect and the highly ordered regions were identified as artifacts from the preparation of thin films required for electron microscopy. In accordance with this finding a series of x-ray studies on amorphous BPA-PC [4–9] indicated that the structure is dominated by intramolecular correlations and that intermolecular correlations involve only directly neighboring chains. These results were obtained by measurements of the scattered intensities for higher momentum transfers ($Q = 4\pi \sin v/\lambda < 8$ Å^{-1}, where λ is the incoming wavelength and $2v$ the scattering angle) and, in some cases, subsequent analysis of the radial distribution function as the spatial Fourier transform of the scattering intensity [4, 5, 9]. The most detailed studies of short-range order in BPA-PC were performed by Červinka et al. [10–13]. They measured the neutron scattering intensities of four differently deuterated BPA-PC samples and compared them to calculated intensities for a random distribution of "scattering units" consisting of several monomers in a fixed configuration. Reasonable agreement was found for an arrangement of three parallel segments of two monomers each in a "trans-trans" conformation. However, their comparison appears to be only qualitative since they did not calibrate the measured intensities in absolute units and did not explain how the incoherent scattering was taken into account. Furthermore, the "scattering unit" approach itself seems to be questionable. With the inherent rigidity of its monomer units it is not likely to model the structure of a random arrangement of flexible chain molecules.

As demonstrated by Schärpf and Gabryś in various papers on PMMA and polystyrene [32–35] experimental accuracy is increased by applying spin polarization analysis. This technique can be used for an experimental separation of coherent and (spin) incoherent scattering contributions. Making use of this separation a rather simple and reliable intensity calibration is possible with the incoherent scattering of the sample as an internal standard. Consequently, we performed all experiments presented here with spin polarized neutrons.

In order to improve the macroscopic properties of BPA-PC, e.g., increase the glass transition temperature, the primary structure of BPA-PC has been modified in various ways [36]. Most of those modifications can be grouped into two classes: either the bisphenol is altered by substitution of certain chemical units or the carbonate group is replaced thus arriving at aromatic polyethers containing for instance a carbonyl or a sulfonyl group. Both types of modification can have a drastic impact on the properties of the polycondensate such as the glass temperature and the mechanical properties.

These correlations between the primary chemical structure and the macroscopic properties of polycondensates have been investigated in a larger research project comprising computer simulations as well as various experimental techniques such as dynamic-mechanical spectroscopy and the neutron scattering experiments described here. First results obtained in the context of this project are reported in [37]. One of the main questions posed there is: do technologically important properties of the polymer glass like toughness and yielding behavior correlate with the microscopic structure of the undeformed solid? Atomistic simulation of the solid in full chemical detail, often known as the "amorphous cell" method, serves as a microscopic model for the polymer glass [38, 39].

The capability of such simulations to answer questions which cannot be directly addressed by experiment as well as the possibility of easy parameter alteration justifies its usefulness for polymeric glasses. The pioneering work of Theodorou and Suter [38], Rigby and Roe [40], and of Clarke and Brown [41] proved, that atomistic simulation in fact can be applied to systems of such a complexity. Since that time the amorphous cell method [38] or the molecular dynamics method for polymer chains in the melt or glassy state [40, 41] has been applied to a variety of polymers and has become a standard tool which is even offered by commercial software packages like *DISCOVER* or *CERIUS*.

Nevertheless, atomistic polymer simulation has to deal with the problem of broad length and time scales. Polymeric structure is first exhibited on a length scale of a bond length (of the order of 1 Å). The typical value of the persistence length (of the order of 10 Å) is the next relevant length characterizing polymers. Finally, we end up with the typical extension of the end-to-end distance or radius of gyration (of the order 100 Å) so that we

cover two orders of magnitude, exhibiting structure and (single) chain properties. This extension of relevant length scales can of course be even much larger, if phase separations become important. The extension of the relevant time scales is much more dramatic, ranging from bond angle vibration ($\approx 10^{-13}$ s) to typical reorientation rates of torsion ($\approx 10^{-11}$ s) and extremely slow processes on macroscopic time scales. The entangled melt viscosity of polycarbonates, for example., suggests at a temperature 50 K above the glass transition temperature and for a polymerization degree of $N = 100$ chain relaxation times in the order of 10^{-3} s. Working with a molecular dynamics time step of integration of one or two orders of magnitude smaller than the fastest relevant oscillation period, one would have to propagate the melt simulation over 10^{12} to 10^{13} steps for only one system at one temperature. This is, of course, clearly beyond today's computer capability. The lack of computer time is indeed not the only problem arising from this enormous spread of time and length scales. Furthermore, we can expect that important phenomena might be hidden in the enormous data material one would gain out of such extremely long runs and that it could be very difficult to filter out the relevant information. Realizing these two obstacles leads to the need of development of coarse grained models [42, 43].

If, on the other hand, one wants to retain atomistic information, one has to introduce some drastic approximations. It is therefore of urgent need, to compare the results of atomistic polymer simulations with experiments revealing information on the local structure.

Neutron scattering provides such a powerful tool. The coherent scattering cross-section as a function of the scattering vector Q can be straightforewardly calculated from the model structures. These cross-sections are then compared to the experimental results. To make such a test more significant both the experiment and the calculation can be performed for different levels of deuteration by using selectively deuterated samples as in Červinka's and Fischer's work [11]. By this variation of the scattering contrast different pair correlations are emphasized for each degree of deuteration, yielding a set of qualitatively different cross-sections for just *one* structure. If a model structure fails to reproduce the cross-sections of all differently deuterated versions of one material it cannot be entirely correct. Discrepancies between experiment and calculation may hint at deficiencies of the "amorphous cell" method. First studies following this concept, which were restricted to undeuterated polycarbonates with different bisphenols, are published in [44].

This paper presents measurements of the elastic coherent cross-sections of BPA-PC and two other polycondensates of bisphenol A, all in four differently deuterated versions. The experimental results are compared to calculated cross-sections of the corresponding "amorphous cell" model structures. It will be demonstrated that the method of spin polarization analysis enables a quantitative comparison of experiment and calculation without any adjusting of the measured intensities to calculated values.

Experimental section

The neutron scattering measurements were performed with differently deuterated samples of three polycondensates of bisphenol A, namely BPA-polycarbonate, BPA-polyether-ketone (BPA-PEK), and BPA-polyethersulfone (BPA-PES), which were supplied by the chemical laboratories of the Bayer AG in Uerdingen. Schematic graphs of the repeat units of all three polycondensates – regardless of their deuteration – are given in Fig. 1. The bisphenols were synthesized following the procedure described in [45] which renders well defined deuterations by the use of deuterated phenol, acetone or hydrochloric acid. By an appropriate polycondensation reaction, for instance, a phosgenation in the case of polycarbonates, the bisphenol and the condensate group are linked to form polymer chains. The differently deuterated versions are schematically sketched in Fig. 2 with their denotations used in the following. The degrees of deuteration, i.e., the share of deuterium in the supposedly deuterated hydrogen positions, were determined by ^{1}H-NMR and found to be in the range between 89.5% (Da-BPA-PES) and 97.0% (Di-BPA-PEK). The molecular weights were determined by the intrisic viscosities method and GPC. They ranged from 12000 g/mol (Da-BPA-PEK) to 80000 g/mol (D-BPA-PC) with M_w/M_n in the range of 1.5 to 2. The bisphenol and all samples have been purified by several subsequent precipitation steps.

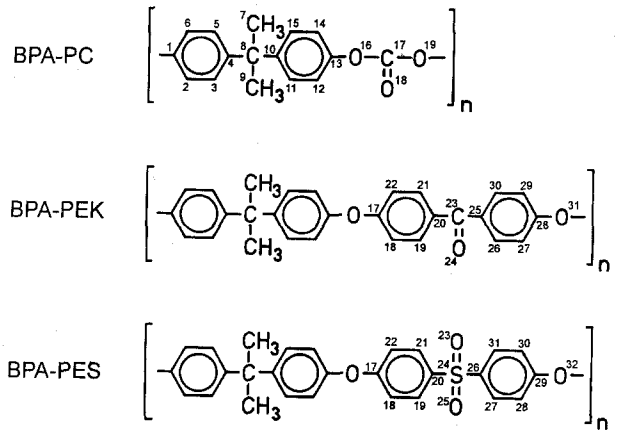

Fig. 1. Repeat units of the different polycondensates of bisphonel A, with carbonate (BPA-PC), ketone (BPA-PEK) or sulfone (BPA-PES) condensate groups. The atomic charges as calculated by the semiempirical MNDO method are for BPA-PC: H_2, H_6, H_{12}, H_{14}: 0.01; C_2, C_6, C_{12}, C_{14}: − 0.04; C_4, C_{10}: 0.02; C_1, C_{13}: 0.18; C_8: 0.05; C_{17}: 0.53; O_{16}, O_{19}: − 0.25; O_{20}: − 0.36; for BPA-PEK: C_2, C_6, C_{12}, C_{14}, C_{18}, C_{22}, C_{27}, C_{29}: − 0.03; C_1, C_{13}, C_{17}, C_{28}: 0.18; C_{23}: 0.25; O_{24}: − 0.25; O_{16}, O_{31}: − 0.24; for BPA-PES: C_1, C_{13}, C_{17}, C_{28}: 0.14; C_{19}, C_{21}, C_{26}, C_{30}: 0.09; C_{20}, C_{26}: − 0.05; O_{16}, O_{32}: − 0.28; O_{23}, O_{25}: − 0.25. S_{24}: 0.24; all other atoms carry negligible charges

For the neutron scattering experiments the glassy samples were hot pressed to hollow cylinders with a length of 5 cm, an outer diameter of 1 cm, and a wall thickness of typically 0.2 mm, with the exception of two substances which were prepared as powder samples. The samples were enclosed in thin aluminum containers which were mounted on the cold finger of a closed-cycle refrigerator or a cryostat and cooled to 10 K or less. At this temperature all atomic motions except for vibrations should be frozen in. Thus, the scattering of the sample is almost entirely elastic with small deviations at higher Q which can be corrected for by a Debye–Waller factor.

The experiments were performed with the triple axis spectrometers HB-1 (Oak Ridge National Laboratory) and H4m (Brookhaven National Laboratory). Both spectrometers are installed directly at the reactor core and supplied with thermal neutrons. By using polarizing monochromator and analyzer crystals such as ^{57}Fe (HB-1) or Heusler alloys (H4m), magnetic spin-flipping coils and guide field, these spectrometers were equipped for spin polarization analysis. With this instrumentation the scattering intensities in spinflip mode, where the neutrons reverse their spin direction in the scattering process, and nonflip mode (scattered neutrons maintain their spin direction) can be separated. In this way spinflip and nonflip intensities were measured in the elastic mode (energy resolution $\Delta E < 2.0$ meV) as a function of the modulus of momentum transfer Q in the region $0.2\,\text{Å}^{-1} \leq Q \leq 2.5\,\text{Å}^{-1}$. Since the measurements did not require a high resolution in Q, but suffered from intensity problems caused by the spin polarization set-up, the widest collimations available with accepted horizontal divergencies of typically 1° were used.

Data analysis

The measured intensities were corrected for background scattering by subtraction of a measurement with an empty sample container, but otherwise identical configuration. For lower

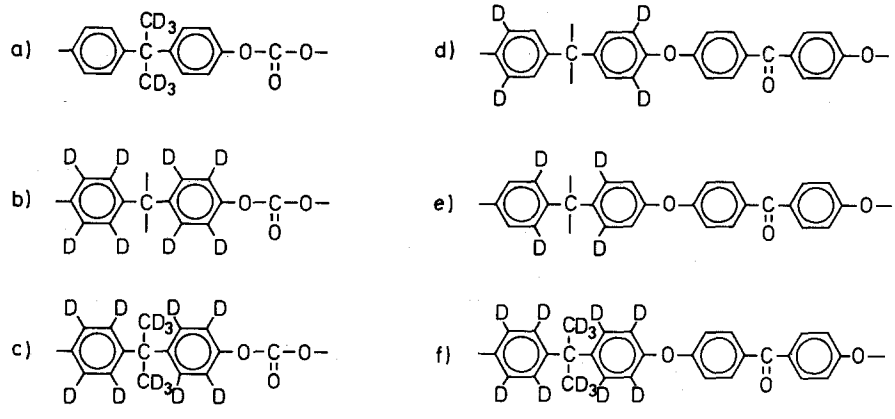

Fig. 2. Differently deuterated versions of polycondensates. a) DAc-BPA-PC, b) DPh-BPA-PC, c) D-BPA-PC, d) Da-BPA-PEK, e) Di-BPA-PEK, f) D-BPA-PEK, the polyether-sulfones correspond to the polyetherketones d)–f) with the sulfonyl instead of the carbonyl group

momentum transfers ($Q < 0.8$ Å^{-1}) a high background was observed due to the rather wide collimation. This effect makes the data in the lower Q region somewhat uncertain, in particular the HB-1 data with low counting statistics and, accordingly, an unfavorable signal-to-noise ratio.

Due to the limited efficiency of the polarizer and the analyzer which transmit a certain share of the "wrong" spin direction the measured intensities had to be corrected for the finite flipping ration R of the spin polarization set-up. The flipping ratio is defined as the ratio of the nonflip and the spinflip intensity for a purely coherent scatterer which should be infinite for a perfect polarization set-up. At the HB-1 a flipping ratio of $R \approx 7$ was measured in the direct beam, whereas the H4m showed a higher value of $R \approx 26$. Following Schärpf's concept [32] the data were corrected for this effect by

$$\hat{I}_{NF} = I_{NF} + \frac{1}{R-1}(I_{NF} - I_{SF}) \quad (1)$$

$$\hat{I}_{SF} = I_{SF} - \frac{1}{R-1}(I_{NF} - I_{SF}) \quad (2)$$

Particularly for samples with a lower transmission, multiple scattering can falsify the results of this kind of experiment: neutrons which have been scattered twice with spinflip have their original spin direction and are therefore registered in the nonflip intensity. For a correction of this effect, the share of multiple scattering was estimated by a computer simulation of the elastic incoherent scattering. In this simulation the reminding path length d after entering the sample or after a scattering process is calculated for the hollow-cylinder geometry of the sample. The scattering probability is then computed by $w = \exp(-\sigma_{inc} nd)$ with σ_{inc} as the total incoherent cross-section per monomer and n as the density of monomers. If w is smaller than a random number z, the neutron is scattered again in the simulation; for $w > z$ the neutron is registered under the angle after its last scattering process. This simulation rendered estimations for the share of multiple scattering as a function of the scattering angle 2ϑ. However, even for the undeuterated BPA-PC sample with its rather low transmission of $T_p = 78\%$ no systematic dependency of the multiple scattering from 2ϑ could be found, so that for a given sample a constant share of double scattering m was assumed for all 2ϑ or Q. The correction was then performed using

$$I^{NF}_{corr} = I^{NF} - \frac{I^{NF}}{\frac{3}{m} - 1} \quad (3)$$

and the corresponding expression for I^{SF}_{corr}. The index "corr" is omitted for clarity in the following.

To account for the attenuation of the elastic scattering by inelastic processes a Debye–Waller factor was included to describe the spinflip intensity

$$I_{SF}(Q) = I^{(0)}_{SF} \cdot \exp(-\tfrac{1}{3}\langle u^2\rangle Q^2) . \quad (4)$$

The latter is due to purely incoherent scattering and thus is Q-independent except for the Debye–Waller factor. The mean-squared displacement $\langle u^2\rangle$ and the intensity $I^{(0)}_{SF}$ were determined by a least-squares-fit of Eq. (4) to the corrected spinflip intensities. The result for Da-BPA-PES (a polyethersulphone with an analogous deuteration pattern as Da-BPA-PEK in Fig. 2) is shown in Fig. 3. This figure demonstrates the reliability of the separation of coherent and incoherent scattering in so far as the corrected spinflip intensity is indeed completely featureless. Table 1 shows the mean-squared displacement $\langle u^2\rangle$ as obtained from the fitting procedure for each sample.

Making use of [46],

$$I_{NF} = I_{coh} + \tfrac{1}{3} I_{inc} \quad (5)$$

$$I_{SF} = \tfrac{2}{3} I_{inc} , \quad (6)$$

the desired quantity, the elastic coherent cross-sections as a function of the modulus of the momentum transfer Q, were calculated by

$$\left(\frac{d\sigma}{d\Omega}\right)_{coh} = \frac{2}{3}\left(\frac{d\sigma}{d\Omega}\right)_{inc} \frac{I_{NF} - \frac{1}{2} I_{SF}}{I_{SF}} , \quad (7)$$

according to the procedure outlined by Schärpf and co-workers in [34]. In Eq. (7) the separation of nonflip and spinflip scattering is utilized in two ways: first, the coherent intensity is separated by $I_{coh} = I_{NF} - I_{SF}/2$ in the denominator of the fraction in Eq. (7), which follows from Eqs. (6) and (5). Secondly, the coherent intensity is calibrated in absolute units, dividing it by the incoherent intensity obtained from Eq. (6) as $3/2 \cdot I_{SF}$ and multiplying it with the incoherent cross-section $(d\sigma/d\Omega)_{inc}$ of the sample. The latter is calculated

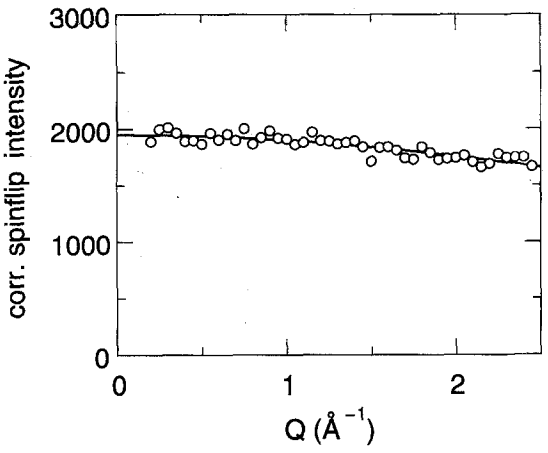

Fig. 3. Spinflip intensities I_{SF} corrected for background, flipping ratio, and double scattering of the polyethersulfone sample with the 2,6-deuterated bisphenol unit (Da-BPA-PES). The solid line is the fit of Eq. (4) to the experimental data

Table 1. Mean-squared displacement $\langle u^2 \rangle$ determined by fitting a Debye–Waller law to the corrected spinflip intensities for each sample.

Sample	Temperature (K)	$\langle u^2 \rangle$ (Å^2)
H-BPA-PC	10.0	0.119
DAc-BPA-PC		0.202
DPh-BPA-PC		0.286
D-BPA-PC		0.074
H-BPA-PEK	1.5	0.063
Da-BPA-PEK		0.067
Di-BPA-PEK		0.125
D-BPA-PEK		0.047
H-BPA-PES	4.2	0.068
Da-BPA-PES		0.077
Di-BPA-PES		0.059
D-BPA-PES		0.072

from the chemical composition taking the degree of deuteration into account. By this internal calibration typical problems arising from the use of an *external* standard can be evaded, for instance, the difference in the effective number of scattering atoms between the sample and the calibration standard. Thus, the separation of nonflip and spinflip intensity by spin polarization analysis enables a rather simple and unambiguous calibration of the coherent scattering cross-section in absolute units.

Figures 4, 5, and 6 show the cross-sections as determined experimentally by the data processing described above. The cross-sections of the undeuterated versions are very similar to those of our previous work on amorphous polycondensates [44], one of which is shown in Fig. 4a for comparison. They also resemble the results of Červinka et al. [10–13] and the diffraction patterns obtained from x-ray experiments [4, 5, 9]. The predominant features are a small peak centered around $Q = 0.5$ Å^{-1} and a strong maximum at about $Q = 1.2$ Å^{-1}. The former can be ascribed to correlations along the backbone of one polymer chain [8], the latter is the so-called "amorphous-halo" which is mostly due to correlations between neighboring chains [6, 8, 9]. Analysis of the peak positions Q_p and the peak widths ΔQ (FWHM assuming a Gaussian line shape) yields estimates for the distance $D_p = 2\pi/Q_p$ between neighboring chains and the corresponding correlation lengths $\xi = 2\pi/\Delta Q$. Similar values are found here and in our previous work cited above, i.e., $D_p \approx 5$ Å and ξ in the range of 20 to 30 Å.

In the case of BPA-PC the use of samples either with deuterated methyl groups (DAc-BPA-PC), deuterated phenylene groups (DPh-BPA-PC) or both (D-BPA-PC) has produced a set of significantly different cross-sections. Most remarkable here is the rather weak and poorly structured scattering from the fully deuterated sample.

In the case of BPA-PEK and BPA-PES the scattering cross-sections of differently deuterated polymers look similar with the exception of the species with the fully deuterated bisphenol unit. This sample produces an intense and rather sharp feature in the coherent cross section at $Q = 0.45$ Å^{-1}.

Simulations

As mentioned in the introduction, the generation of glassy polymer models necessarily implies some drastic approximations. The most important problem to overcome is the lack of computer time to simulate realistic quenching rates from the melt. There is no evident way to circumvent this problem and, therefore, a variety of approaches has been described in the literature: Starting from vacuum RIS (Rotational Isomeric State) chains [47], modifying the RIS scheme [38, 48], using

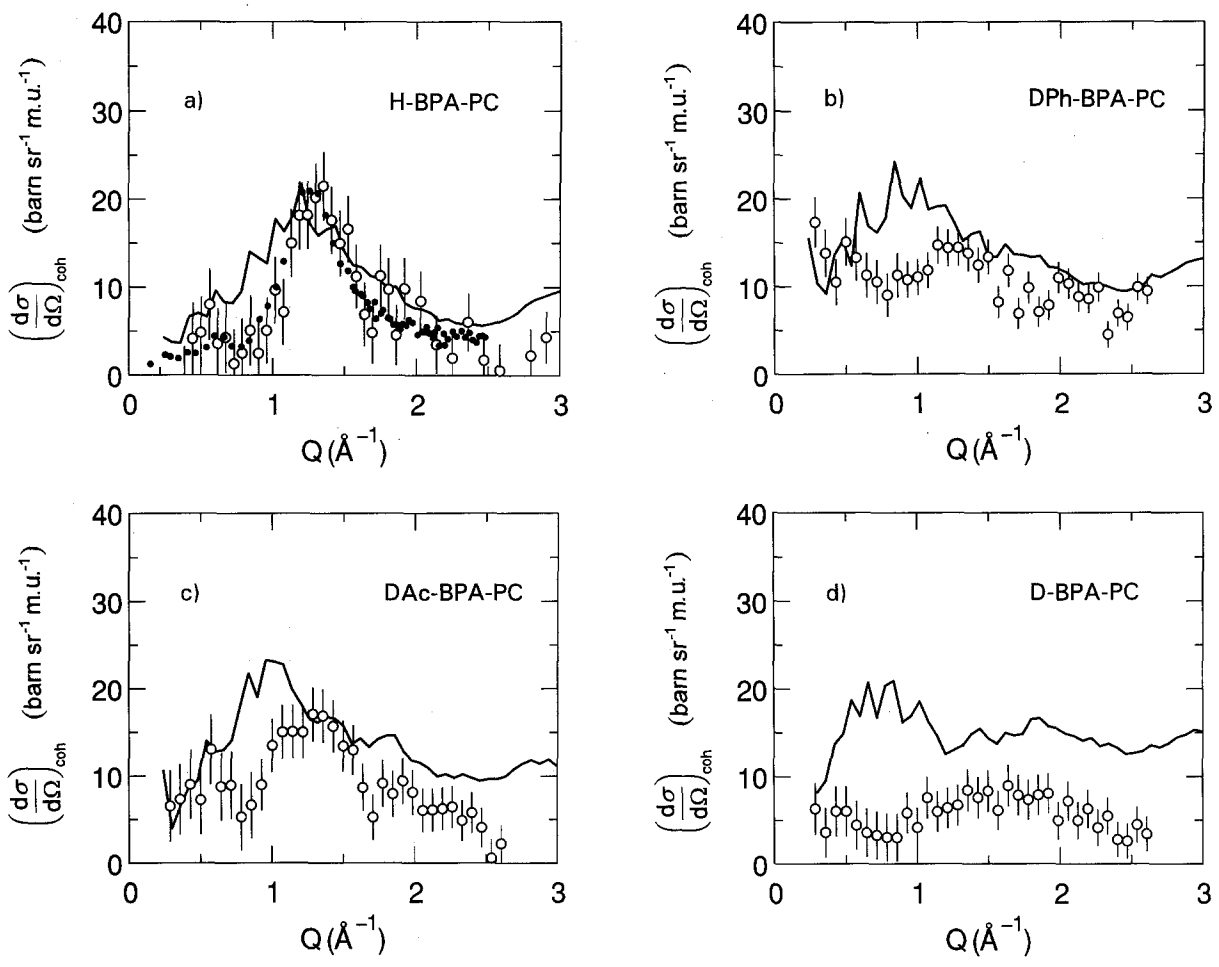

Fig. 4. a)–d) Comparison of elastic coherent cross-sections of BPA-PC, measured with spin polarized neutron scattering (○). To confirm the reliability of the rather weak data a previous measurement on the powerful D7 spectrometer of the ILL Grenoble has been added as dots [44]. The values resulting from the "amorphous cell" simulations are represented by the solid line which simply connects the calculated values by straight lines

Continuum Configurational Bias Monte Carlo [49], molecular dynamics with soft core potentials [50-52] or the *dynamic Monte Carlo* method [53], building single chain conformations by the *PRISM* theory [54], connecting randomly placed monomers to build a chain [55], relaxing by local rotations [56] are all methods which have been proposed and realized. In this work, we have adopted a procedure which is only slightly different from the original energy minimization method proposed by Theodorou and Suter [38, 39]. The complexity of the chemical structure of the systems studied implies very high quenching rates if one would use methods like molecular dynamics or Monte Carlo, i.e., if one would introduce a temperature. Thus the chain motion would be mainly dominated by the potential energy and not the kinetic energy. We therefore expect no major improvement from such approaches for our systems as long as one has to confine oneself to computer runs of moderate length (a couple of weeks on a CONVEX 220).

The energy E of our systems is given by

$$E = E_{\text{Coulomb}} + E_{\text{NB}} + E_{\text{Torsion}} \,. \tag{8}$$

E_{Coulomb} is the Coulomb energy of the system, E_{NB} is the non bonded energy given by a 12-6 Lennard Jones Potential with the parameters of the *AMBER* force field [57] and E_{Torsion} is the torsional potential.

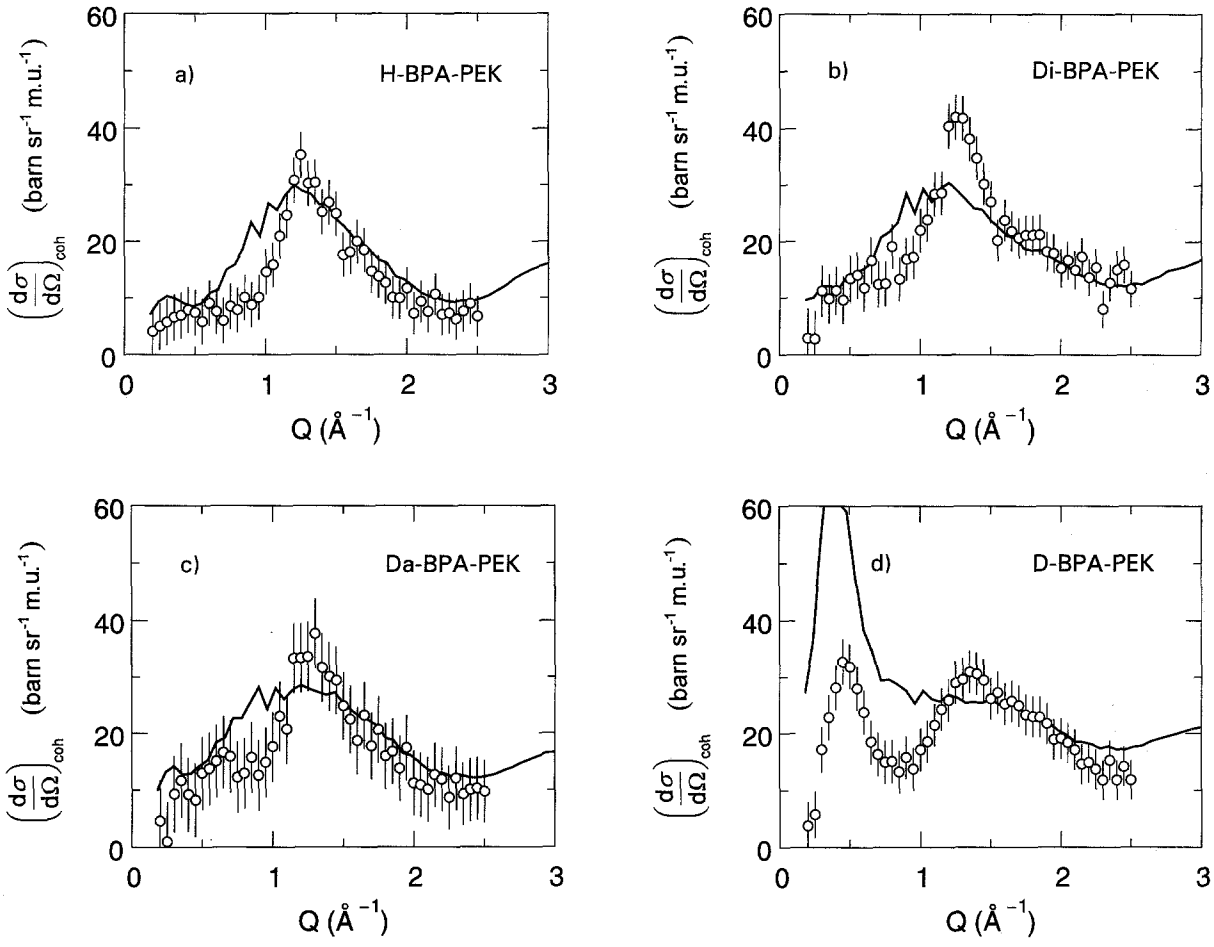

Fig. 5. a)–d) Comparison of elastic coherent cross-sections of BPA-PEK, measured with spin polarized neutron scattering (○) and calculated from "amorphous cell" model structures (solid line)

The partial charges were determined by a semi-empirical MNDO (Modified Neglect of Differential Overlap) calculation (see Fig. 1). This calculation gives the following approximate picture for the charge distribution along the chain:

1) The phenyl quadrupoles seem to be negligible.
2) The strongest interaction present is given by the carbonyl of the PEK group which is clearly a dipole.
3) The ether group gives rise to a quadrupole moment.
4) The sulfonyl and the carbonate moieties show a more complicated behavior. On short scales they are not neutral and should therefore couple to the quadrupoles present. On longer scales on the other hand one does not expect a significant interaction.

We should not forget at this point that polarizabilities are taken into account only on an atomic scale by the Lennard–Jones potentials. They are (as usual in force field descriptions) omitted on a molecular level. Nevertheless, phenylene ring polarizabilities might be important.

As in the work of Hutnik et al. [39], we do not restrict ourselves to the accuracy of general purpose force fields for the torsion potentials, but we prefer to determine the force field torsion parameters which separately fit each molecule best. If one is interested in vacuum conformations general force fields are acceptable since there, generally, one does not expect an appreciable

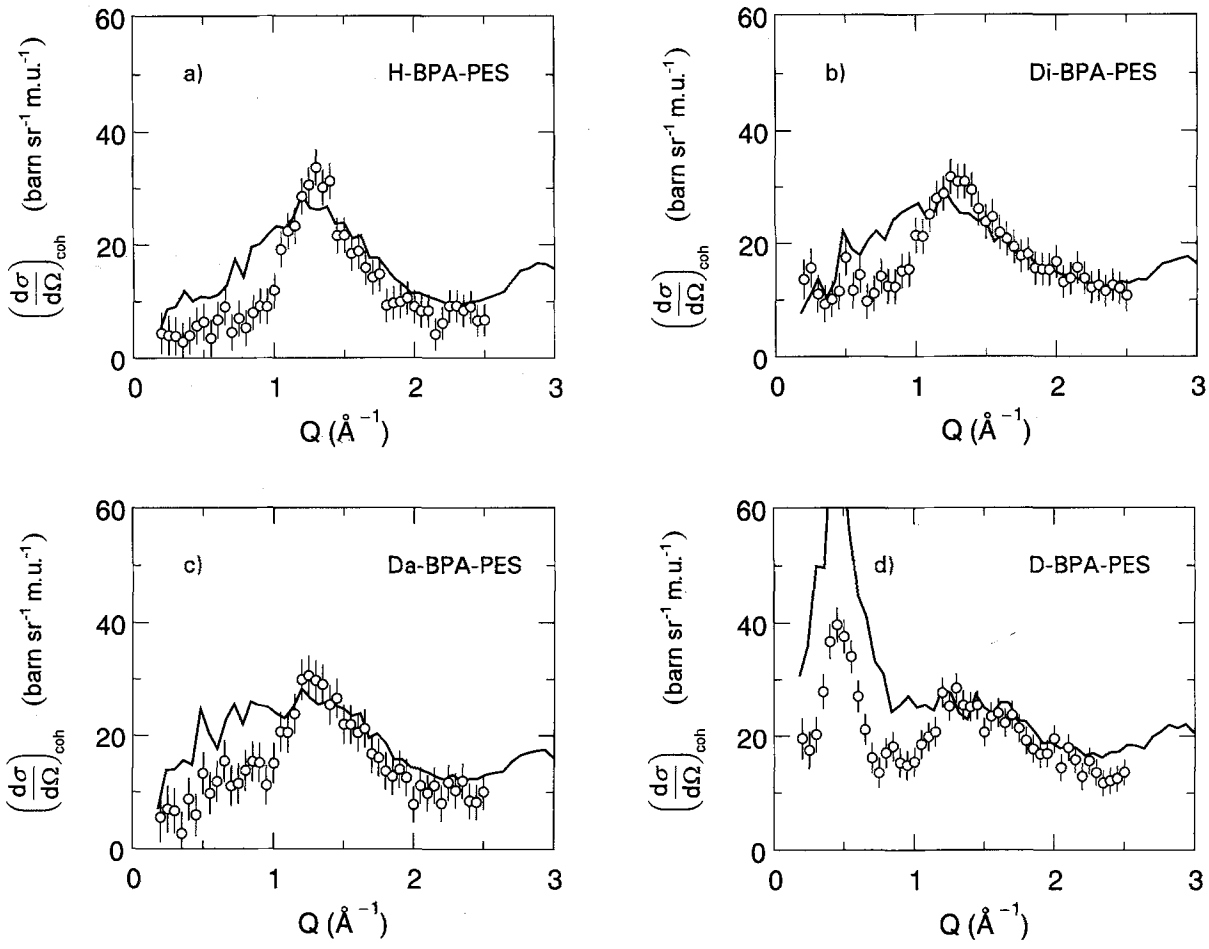

Fig. 6. a)–d) Comparison of elastic coherent cross-sections of BPA-PES, measured with spin polarized neutron scattering (○) and calculated from "amorphous cell" model structures (solid line)

deviation from the equilibrium geometry. In dense systems, however, frequent deviations around this equilibrium geometry are expected and therefore one has to know the curvature around the potential minimum to a sufficient accuracy. We therefore determined the torsion potentials by ab initio calculations (GAUSSIAN 90 [58]) with the basis set 6-31G for all molecules except for the polysulfone where we adopted a 6-31G* basis set. We used 2,2-diphenylpropane, monophenylcarbonate, and diphenylcarbonate as model structures for the potentials of BPA-PC, 2,2-diphenylpropane, diphenylether, and benzophenone as model structures for the potentials of BPA-PEK and, finally, 2,2-diphenylpropane, diphenylether, and diphenylsulfone as model structures for the potentials of BPA-PES. The potentials are shown in Figs. 7–9. A detailed description of these calculations will be given elsewhere [59]. The results of the calculations can be qualitatively summarized as follows:

1) The rotation around the bond between the phenylene carbon and the backbone oxygen is almost free (see Fig. 8)
2) The barrier of ring flips is therefore mainly determined by the barrier of the rotation opposite to the aforementioned bond with respect to the ring. This latter barrier is approximately 2 kcal/mol in the case of 2,2-diphenylpropane, 2 or 3 kcal/mol, respectively, in the case of benzophenone and 4 kcal/mol in the case of diphenylsulfone.
3) The highest barrier is given by the trans-

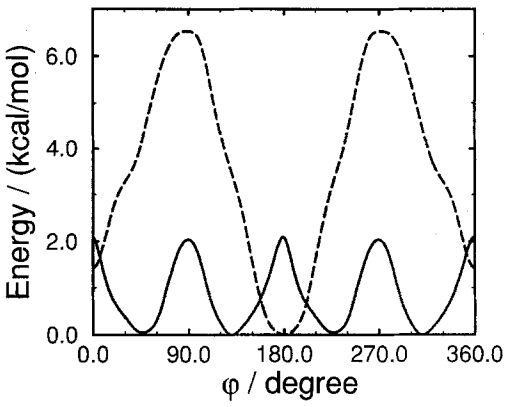

Fig. 7. Ab initio 6-31G torsion potential of 2,2-diphenylpropane (full line) defined by the atoms 4, 8, 10, 11, and of diphenylcarbonate (dashed line) defined by the atoms 13, 16, 17, 19. The enumeration refers to Fig. 1, BPA-PC

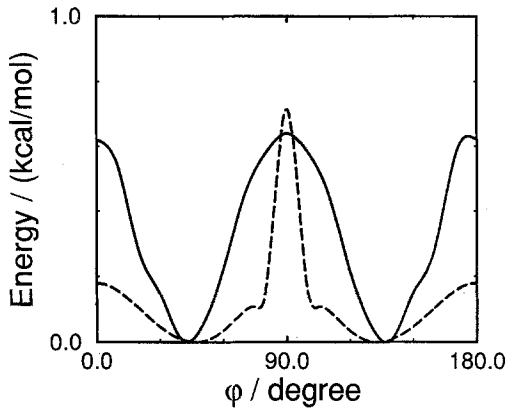

Fig. 9. Ab initio torsion potential of benzophenone (6-31G, full line) defined by the atoms 21, 20, 23, 25 (see Fig. 1, BPA-PEK) and of diphenylsulfone (6-31G*, dashed line) defined by the atoms 21, 20, 24, 26 (see Fig. 1 BPA-PES)

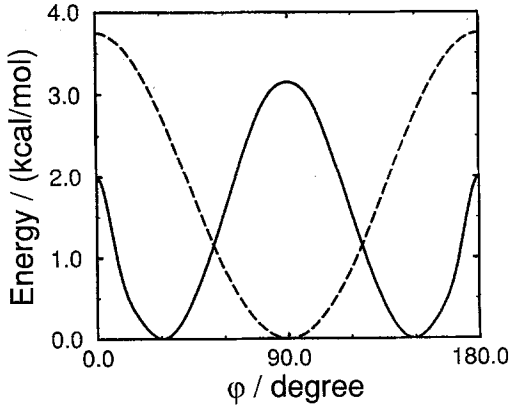

Fig. 8. Ab initio 6-31G torsion potential of monophenylcarbonate (full line) defined by the atoms 14, 13, 16, 17, (see Fig. 1, BPA-PC) and of diphenylether (dashed line) defined by the atoms 12, 13, 16, 17 (see Fig. 1, BPA-PEK)

trans to trans-cis flip of the carbonate moiety (6.5 kcal/mol)

In all three cases, we simulated a system of 12 chains with a polymerization degree $N = 6$. We avoided using only one chain in order to gain some more flexibility during the minimization. The tradeoff is, however, that since the exact experimental system density is only known for long chain systems, using short chains probably leads to slightly too high densities of our system. These (long chain system) densities ($\rho^{BPA-PC} = 1.19\ g/cm^3$, $\rho^{BPA-PEK} = 1.16\ g/cm^3$, $\rho^{BPA-PES} = 1.23\ g/cm^3$) translate to system sizes of roughly 30 Å for BPA-PC and 35 Å for BPA-PEK and BPA-PES. These volumes were kept fixed during the simulation.

Special care has to be taken of the determination of the starting conformations. Very often the potential effective during the chain growth includes the non bonded interactions [38, 39] and the growth algorithm resembles a biased sampling Rosenbluth–Rosenbluth method [60, 61] without correction for the bias. This leads to almost overlapping free conformations for the first monomers of the chain. Overlaps cannot be avoided at the later growth stages where the box density has almost reached its final value. Although this approach leads to not too high non bonded energies at the minimization start, it introduces a bias: The chain ends are more coiled than the first monomers since the latter grew in an almost monomer free environment. To avoid this artifact, we preferred to use only the torsion potential during the growth, including information on the nonbonded interaction only on a very local scale along the chain backbone: Interdependencies of consecutive torsions were taken into account by constructing the "Ramachandran" energy profile. Thus, the statistics of the chains resemble that of a non reversal random walk [61] or an RIS model with torsions defined continuously.

Assuming that the persistence length of the chains in the melt at a temperature T near the glass transition temperature T_g is more or less

equal to that given by our RIS-like method in vacuum at that temperature, we only have to "repair" the huge nonbonded energies on a *local* scale. This is done in a way very similar to that of Kremer and Grest [51] or McKechnie et al. [52]: The amplitude of the non bonded interaction grows from 1/1000 of its full value linearly on a logarithmic scale within 12 steps to its full value. Throughout this procedure the torsion potentials remain fixed at their full value. Although we are aware of the fact that this method is much more efficient in a molecular dynamics or in a Monte Carlo simulation, where a temperature is defined, we expect also in a simple minimization a better leveling off of the density fluctuations present at the start of the simulation. Each minimization ran until the system gradient divided by the degrees of freedom reached a value of about 0.05 to 0.005 kcal/mol. Further iterations did not result in a better agreement to the experimental scattering functions. By this procedure, five model structures of BPA-PC, 10 of BPA-PEK and three of BPA-PES have been generated.

Discussion

The experimental results will be discussed and interpreted mainly by a comparison with calculations obtained from "amorphous cell" computer simulations. For a given model structure, i.e., a set of atomic positions $\underline{R}_j$ in a box with the edge lengths L_x, L_y, and L_z, the scattering cross-section per monomer unit (*m. u.*) can be calculated by

$$\left(\frac{d\sigma}{d\Omega}\right)_{\text{coh}}(Q) = \frac{1}{N_{\text{m.u}}}\left\langle \left| \sum_j b_j \exp(\mathrm{i}\underline{Q}\cdot\underline{R}_j)\right|^2 \right\rangle_{\underline{Q}} \quad (9)$$

Since the scattering cross-section for unoriented solids depends only on the modulus of $\underline{Q}$, the calculated $(d\sigma/d\Omega)_{\text{coh}}$ have to be averaged over all $Q = |\underline{Q}|$, which is denoted by $\langle\cdots\rangle_{\underline{Q}}$ in Eq. (9). $N_{\text{m.u.}}$ is the number of monomer units in the cell. Due to periodic boundary conditions for the model structures, the elastic cross-section as the spatial Fourier transform of the pair correlation function is defined only for those discrete points $\underline{Q} = (Q_x, Q_y, Q_z)$ in reciprocal space which obey $Q_x = 2\pi n_x/L_x$ (analogous for Q_y, Q_z), where the n_x, n_y, n_z are zero or positive integers.

For all of the aforementioned model structures the neutron scattering cross-sections have been calculated and averaged over all structures separately for each deuterated version. For the choice of the scattering lengths b_j in Eq. (9) the kind of deuteration as given in Fig. 2 has to be taken into account.

Figures 4 to 6 show the comparison of the neutron scattering cross-sections of the three BPA polycondensates – each in four differently deuterated versions – on the one hand measured in the experiment, and on the other hand calculated from the "amorphous cell" model structures. The calculated values are represented by straight lines connecting individual points such that the sharp peaks at lower Q values represent the statistical accuracy and are by no means true features. It should be noted here that the intensity calibration provided by spin polarization analysis enables a direct comparison between experimental and calculated cross-sections without any arbitrary adjusting procedures.

The agreement between experiment and simulation still seems unsatisfactory for BPA-PC (see Fig. 4) but for BPA-PEK and BPA-PES (Figs. 5 and 6) at least some qualitative similarity can be recognized. However, especially on larger length scales, i.e., at lower values of Q, the cross-section $(d\sigma/d\Omega)_{\text{coh}}$ is systematically higher in the simulation than it is in the experiments. At the same time, the height of the amorphous halo is slightly underestimated in the simulations, whereas its width comes out significantly too high.

As outlined before, contrary to previous studies, "amorphous cell" assumes a "random coil" conformation and does not anticipate any structural order such as clusters of parallel chain segments. The qualitative agreement between experiment and "amorphous cell" results thus supports the validity of the "random coil" concept valid for polycarbonate and the other polycondensates, in accordance with the observations in previous scattering experiments [4–9]. However, the significant deviations for smaller momentum transfers indicate that on larger length scales the computer modeling becomes increasingly incorrect. This is also reflected in the overestimation of the widths of the strong maxima at $Q \approx 1.2\ \text{Å}^{-1}$ for undeuterated samples, the so-

called "amorphous halos," which has already been observed in previous work on undeuterated polycarbonates [44]. In that study, an insufficient structural relaxation was assumed as the cause for this underestimation of correlation lengths. In order to facilitate the relaxation of the "quenched" initial configuration the "amorphous cell" algorithm has been modified in two ways compared to the work in [44] (see previous section for details):

1) the potentials of the non-bonded interaction do not have their full height from the beginning, but are slowly increased during the relaxation process
2) the cell is filled with several shorter chains instead of one long chain

As outlined in the previous section, both modifications should enable the system to withdraw from the extreme non-equilibrium initial configuration more easily. Nevertheless, the amorphous halos in the calculated cross-sections of the H-BPA-PC, -PEK and -PES samples are still too broad compared to the experiment, although they are significantly narrower than those obtained from the original "amorphous cell" version in [44]. However, we must be aware of the fact that "amorphous cell" cannot be expected to correctly reproduce correlation lengths which are hardly smaller than the cell size. Here, as well as in our previous work [44], correlation lengths for the packing of neighboring chains up to $\xi = 28$ Å are found. These, however, come very close to the dimensions of the "amorphous cell" cubes of 30 Å and 35 Å, respectively.

Furthermore, the comparison between measured and calculated cross-sections shows peaks at $Q \approx 0.9$ Å^{-1} (DAc-BPA-PC and DPh-BPA-PC) and at $Q \approx 1.8$ Å^{-1} (DAc-BPA-PC) in the simulation, which are not reflected in the experiment. In the case of D-BPA-PEK and D-BPA-PES (both having fully deuterated bisphenol units) the first peak is shifted from $Q \approx 0.45$ Å^{-1} (experiment) to $Q \approx 0.35$ Å^{-1} (simulation) and is much too intense in the calculation. Possible explanations for these findings will be discussed below.

The most striking discrepancy between experiment and calculation is observed for the fully deuterated D-BPA-PC, where the calculated cross-section is much larger than the measured one in the entire scanned Q region. For an interpretation of this effect, it should be kept in mind that for a fully deuterated sample the diffuse scattering is dominated by the contrast between free volume and volume occupied with atoms, since all scattering atoms (D, C and O) have similar scattering lengths of $b \approx 0.6 \cdot 10^{-12}$ cm. Thus, the overestimation of the scattering from D-BPA-PC suggests that the distribution of free volume in the simulated structures is too uneven compared to the real structures. Accordingly, it can be gathered from the comparison that the "amorphous cell" method as it is currently implemented tends to overestimate the density fluctuations especially on larger length scales. Obviously, this should mainly be attributed to incomplete relaxation. In a recent study of Floudas et al. [22] an average hole size of 6 Å has been derived from small-angle x-ray scattering. This is in rough agreement with the "amorphous-cell" prediction of 3 to 5 Å for the typical diameter of holes and therefore contrary to our own findings.

For a further interpretation of measured and calculated cross-sections and, in particular, the analysis of discrepancies between experiment and calculation, it would be very helpful if features in $(d\sigma/d\Omega)_{\mathrm{coh}}(Q)$ could be ascribed to certain pair correlations. The calculation of elastic scattering cross-sections from "amorphous cell" model structures provides a method for such an interpretation which will be explained in the following.

In the calculation of the cross-section for a given sample according to Eq. (9), "manipulated" values for the scattering lengths ($b_j = 0$ in most cases) can be used instead of the real values. In general, this will yield a change of the calculated cross-section which contributes to the understanding of the underlying pair correlations. To put it more clearly: if the scattering length b_j of the j-th atom is set to zero, this will influence (mostly attenuate) the cross-section at all Q, where pair correlations involving the such labeled atom are significant. This would then lead to the conclusion that a peak at Q_p which is attenuated by this procedure results from a pair correlation involving the atom no. j. Thus, by identifying specific features using the computer-generated structures, it is possible to extract information on the spatial distribution of scattering units in the polymer directly from the measured neutron scattering cross-section.

By a systematic variation of the atoms or atom groups where the scattering lengths are set to zero the observed peaks in $(d\sigma/d\Omega)_{coh}(Q)$ can be ascribed to certain pair correlations. The effectiveness of this approach will be demonstrated here for the undeuterated H-BPA-PEK. In this case two peaks are observed, a smaller one at $Q_p \approx 0.35$ Å^{-1} and the amorphous halo at $Q_p \approx 1.2$ Å^{-1}. As shown in Fig. 10 the small peak disappears if the scattering lengths of the atoms of the carbonyle group are set to zero. The amorphous halo vanishes almost completely if the scattering lengths of all carbon atoms of the polymer backbone are set to zero. As outlined before, the low Q feature can be ascribed to correlations *along* the polymer backbone. Now it can be concluded that it is mainly the correlations between succeeding carbonyle groups at a distance of $2\pi/Q \approx 18$ Å being responsible for this specific peak of BPA-PEK in the scattering cross-section.

A further example is instructive for the understanding of the obvious disagreement at low momentum transfers between experiment and calculation for the bisphenol-deuterated D-BPA-PEK and -PES. Figure 11 demonstrates that the low-Q peak is caused by correlations of the methyl groups. Its height decreases drastically, when the scattering lengths of all atoms in the methyl groups are set to zero. As mentioned before, this peak is shifted from $Q_p \approx 0.45$ Å or $D_p \approx 14$ Å in the experiment to $Q_p \approx 0.35$ Å^{-1} ($D_p \approx 18$ Å) in the calculated cross-section. According to the evidence suggested by Fig. 11 and the value of D_p, it is justified to assume that correlations of subsequent methyl groups along one chain are the origin of this peak. This assumption is confirmed by an analysis of the interatomic distances of our RIS-like chains (see previous chapter), which yields a value of $R_M = (17.6 \pm 2.6)$ Å for the average distance of two subsequent methyl groups in BPA-PEK, in good agreement with the values of D_p for the corresponding peak in the calculated cross-section. The overestimation of this distance and of the peak intensity implies that the simulated chain is too rigid and too stretched compared to the real chain. This might be a consequence of the simulation algorithm where both the bond lengths and the bond angles remain fixed, which imposes an unrealistic stiffness on the chain. The aforementioned peaks at $Q_p \approx 0.9$ Å^{-1} and at $Q_p \approx 1.8$ Å^{-1}, which appear in the calculated cross-sections of DAc-BPA-PC, but not in the measured ones, can be traced back to correlations of the methyl groups, as demonstrated in Fig. 12. In a similar fashion, the peak at $Q \approx 0.9$ Å^{-1} in the calculated cross-section of DPh-BPA-PC which is also not reflected in the experiment could be explained. This peak is due to correlations of those phenylene carbon atoms which are not on the 1,4-axis of the ring, as demonstrated in Fig. 13. In both cases the inter- or intramolecular origin of the correlations could not be distinguished. Thus, it is not yet clear how these obviously "artificial" correlations of certain atom groups come about in the simulation; they might as well be a consequence of the fixed bond angles.

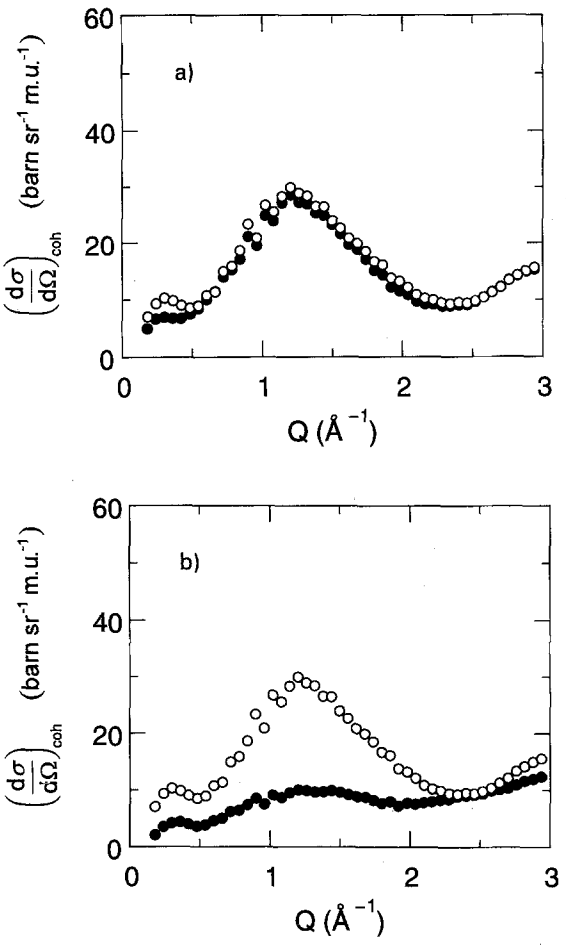

Fig. 10. Calculation of the elastic coherent cross-section of H-BPA-PEK with "true" scattering lengths (○), and with manipulated values (●), here with a) $b = 0$ for the carbonyl and b) b = 0 for the carbon atoms of the backbone

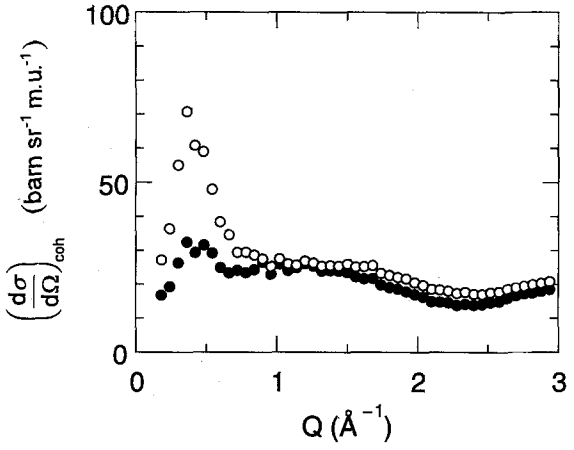

Fig. 11. Calculation of the elastic coherent cross-section of D-BPA-PEK with "true" scattering lengths (○), and with manipulated values (●), here $b = 0$ for the methyl groups

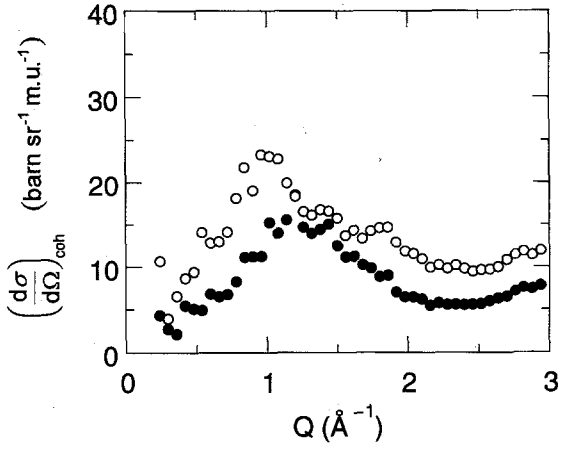

Fig. 12. Calculation of the elastic coherent cross-section of DAc-BPA-PC with "true" scattering lengths (○), and with manipulated values (●), here $b = 0$ for the methyl groups

Summing up the findings from the comparison of cross-sections from neutron scattering experiments on the one hand, and from calculations from "amorphous cell" model structures on the other hand, it can be stated that, by and large, the amorphous polycondensates exhibit a "random coil" conformation without any significant long-ranging intermolecular correlations. However, certain discrepancies between experiment and calculation, i.e., the broadening of the amorphous halos, the overestimation of the scattering from a fully deuterated sample and the shift of peaks to

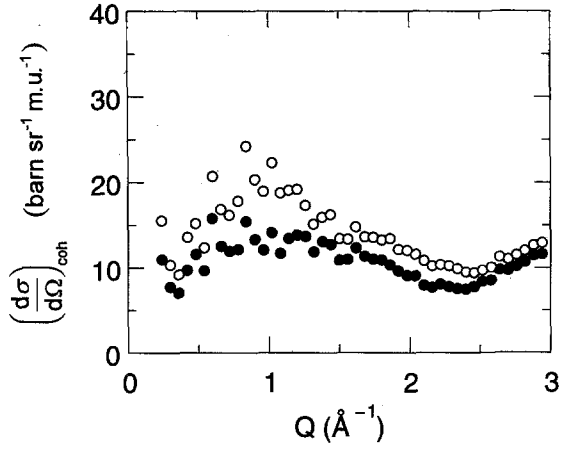

Fig. 13. Calculation of the elastic coherent cross-section of DPh-BPA-PC with "true" scattering lengths (○), and with manipulated values (●), here $b = 0$ for the aromatic carbon atoms in 2, 3, 5 and 6 position of the phenylene groups

smaller momentum transfers reveal an insufficient structural relaxation within the simulation. Also, structural features on larger length scales are not reproduced correctly. This is understandable since the "amorphous cell" approach lacks the necessary relaxation on these scales as a consequence of the melt description with full atomistic detail.

The agreement of our study with a random-coil conformation of the chains in glassy polycondensates can now be compared to the statements of Červinka and Fischer [10–13]. These authors model BPA-PC as an arrangement of three polymer segments containing two repeat units each. These three segments are ordered parallel to each other to account for the relatively high degree of short-range order found in their neutron scattering experiments. However, our results obtained from the "amorphous cell" simulation show no necessity to claim parallely ordered regions over distances as large as 20 Å, the approximate length of two BPA-PC repeat units. Obviously, the reasonable agreement between experiment and calculation in [11] is based on an incorrect method of calculating the scattering intensity for a given structural unit. To account for the so-called "form factor peak" at low Q a rather arbitrary exponential term has been substracted from the calculated intensity. A correct calculation of the scattering intensity for a structural

unit as described by Neumann et al. [62] might yield different results.

How far have the neutron scattering experiments or the simulations reported here contributed to the understanding of correlations between primary structures and macroscopic properties, the major goal of the underlying research project? Up to now, the most enlightening aspect of our work in this context is the comparison between BPA-polyetherketone and -polyethersulfone. Despite their far-reaching resemblance in the primary structure (see Fig. 1), both materials exhibit striking differences as far as the mechanical properties are concerned. BPA-PEK is found to be quite brittle, whereas BPA-PES shows a rather tough behavior similar to BPA-PC. In the "amorphous cell" simulation BPA-PEK and BPA-PES differ in the rotational potential between the phenylene rings of the condensate groups, and in the charge distribution of the carbonyl and the sulfone group. However, these rather small deviations are hardly reflected in the calculated cross-sections for both materials. The only noticeable difference is observed for the undeuterated versions, where H-BPA-PEK displays a peak at $Q \approx 0.3$ Å^{-1}, which is not observed in H-BPA-PES. The measured cross-sections of both polycondensates are even more similar. The comparison of the experimental cross-sections in Figs. 5 and 6 does not reveal any qualitative differences. Obviously, the static structure in BPA-PEK and BPA-PES does *not* provide an explanation for the observed differences in the macroscopic behavior. Consequently, one should focus on the *dynamics* of these systems in the approach to a microscopic understanding of mechanical properties. A systematic combination of quasielastic neutron scattering with dielectric and mechanical relaxation and NMR methods would be a promising challenge for further investigations.

Conclusions

Diffuse neutron scattering has proved to be an appropriate method for the investigation of the static structure and particularly the short-range order in amorphous polycondensates. It turned out to be very helpful to vary the scattering contrast by selective deuteration of hydrogen positions and thus enhance the experimental relevance. It has been demonstrated how spin polarization analysis facilitates a direct comparison of the experimental results to model calculations. To achieve this direct comparison, the incoherent scattering portion had to be removed from the signal and the coherent intensities had to be reliably calibrated to absolute units.

The measured neutron scattering intensities were compared to calculated ones for model structures obtained by "amorphous cell" computer simulations, where the static structures of several polycondensates were modeled by energy relaxation of an initial structure generated by an RIS-like procedure. The qualitative agreement between measured and calculated cross-sections demonstrates that the "random coil" conformation without long-ranging inter-molecular correlations as assumed in the "amorphous cell" simulations is also predominant in the polycondensates investigated here. However, certain discrepancies between experiment and calculation particularly for higher deuterated samples and smaller momentum transfers indicate that the "amorphous cell" method does not reproduce all structural aspects correctly. A detailed analysis of these discrepancies shows that the correlation length for the packing of neighboring chains is underestimated, that the free volume is distributed too unevenly and that the polymer chain is too rigid and too stretched in the simulation. These deficiencies of the "amorphous cell" simulation method should mainly be attributed to an insufficient structural relaxation of the initial configuration and to the local approach of this method, which obviously fails to reproduce structural features on larger length scales. Nevertheless, it is remarkable that a simulation technique which is rather crude in view of the complexity of the underlying physics gives a good approximation of many basic features.

The comparison of BPA-PEK and BPA-PES shows that both materials resemble each other in their diffuse scattering, as expected from their similar primary structures. The significant differences in their mechanical behavior are not reflected in their short-range order and thus must be attributed to different molecular dynamics.

Acknowledgement

This work was supported by Bayer AG and the German Bundesministerium für Forschung und Technologie. Work

at Brookhaven is supported by the Division of Materials Science, U. S. Department of Energy, under Contract No. DE-AC02-76CH00016. Furthermore, we would like to thank Dr. H. Hespe, Dr. B. Pittel, Dr. R. Plaetschke and Dr. K. Sommer from Bayer AG, Prof. K. Binder (Univ. of Mainz), Prof. Suter (ETH Zürich), Prof. D. W. Heermann (Univ. Heidelberg) and Dr. K. Kremer (KFA Jülich) for enlightening discussions and for manifold support in connection with the polycondensate project.

References

1. Prietzschk A (1958) (Kolloid-Z 156:8
2. Hermans PH, Weidinger A (1963) Makromol Chem 64:135
3. Bonart R (1966) Makromol Chem 92:149
4. Wignall GD, Longman GW (1973) J Mat Sci 8:1439
5. Wignall GD, Longman GW (1976) J Macromol Sci Phys B12:99
6. Turska E, Hurek J, Zmudziński L (1979) Polymer 20:321
7. Saffell JR, Windle AH (1980) J Polymer Sci: Polym Lett Edn 18:377
8. Mitchell GR, Windle AH (1985) Coll & Polym Sci 263:280
9. Schubach HR, Heise B (1986) Coll & Polym Sci 264:335
10. Červinka L, Fischer EW (1985) J Non Cryst Solids 75:63
11. Červinka L, Fischer EW, Hahn K, Jiang B-Z, Hellmann GP, Kuhn K-J (1987) Polymer 28:1287
12. Červinka L, Fischer EW (1988) J Non Cryst Solids 106:343
13. Červinka L, Fischer EW, Dettenmaier M (1991) Polymer 32:12
14. Jones AA, Bisceglia M (1979) Macromolecules 12:1136
15. O'Gara JF, Desjardins SG, Jones AA (1981) Macromolecules 14:64
16. Connolly JJ, Gordon E, Jones AA (1984) Macromolecules 17:722
17. Ngai KL, Rendell RW, Yee AF (1988) Macromolecules 21:3396
18. Lee PL, Schaefer J (1992) Macromolecules 25:5559
19. Yee AF, Smith SA (1981) Macromolecules 14:54
20. Morbitzer L, Grigo U (1988) Angew Makromol Chem 162:87
21. Weymans G, Berg K, Morbitzer L, Grigo U (1988) Angew Makromol Chem 162:109
22. Floudas G, Higgins JS, Meier G, Kremer F, Fischer EW (1993) Macromolecules 26:1676
23. Frank W, Goddar H, Stuart HA (1967) J Polymer Sci, Part B: Polymer Letters 5:711
24. Carr SH, Geil PH, Baer E (1968) J Macromol Sci -Phys B2:13
25. Siegmann A, Geil PH (1970) J Macromol Sci -Phys B4:239
26. Siegmann A, Geil PH (1970) J Macromol Sci -Phys B4:273
27. Yeh GSY (1972) J Macromol Sci -Phys B6:465
28. Neki K, Geil PH (1973) J Macromol Sci -Phys B8:295
29. Renninger AL, Wicks GG, Uhlmann DR (1975) J Polymer Sci: Polym Phys Edn 13:1247
30. Fischer EW, Wendorff JH, Dettenmaier M, Lieser G, Voigt-Martin I (1976) J Macromol Sci -Phys B12:41
31. Ballard DGH, Burgess AN, Cheshire P, Janke EW, Nevin A, Schelten (1981) J Polymer 22:1353
32. Schärpf O. in Neutron Scattering in the 'Nineties, Proceedings Series, International Atomic Energy Agency: Vienna, 1985
33. Gabryś B, Higgins JS, Schärpf O (1986) J Chem Soc Faraday Trans. 1 82:1929
34. Schärpf O, Gabryś B, Pfeiffer DG (1990) Short-range Order in Isostatic, Atactic and Sulfonated Polystyrene Measured by Polarized Neutrons, ILL-Report 90SC26T, Institut Laue-Langevin: Grenoble
35. Gabryś B, Schärpf O (1992) Physica B 180 & 181:495
36. Freitag D, Fengler G, Morbitzer L (1991) Angew Chem 103:1626
37. Sommer K (1991) Adv Mat 3:590
38. Theodorou DN, Suter UW (1985) Macromolecules 18:1467
39. Hutnik M, Gentile FT, Ludovice PJ, Suter UW, Argon AS (1991) Macromolecules 24:5962
40. Rigby D, Roe R-J (1987) J Chem Phys 87:7285
41. Clarke JHR, Brown D (1989) Mol Sim 3:27
42. Baschnagel J, Binder K, Paul W, Laso M, Suter U, Batoulis J, Jilge W, Bürger T (1991) J Chem Phys 95:6014
43. Paul W, Binder K, Batoulis J, Pittel B, Sommer K (1993) Makromol Chem Macromol Symp 65:1
44. Lamers C, Schärpf O, Schweika W, Batoulis J, Sommer K, Richter D (1992) Physica B 180 & 181:515
45. Hedrick JL, Dumais JJ, Jelinski LW, Patsiga RA, McGrath JE (1987) J Polymer Sci A: Polym Chem 25:2289
46. Gerlach P, Schärpf O, Prandl W, Dorner B (1982) Journal de Physique 43:C7-151
47. Müller-Plathe F (1991) J Chem Phys 94:3192
48. Brown D, Clarke JHR (1986) J Chem Phys 84:2858
49. Pablo JJ, Laso M, Suter UW (1992) J Chem Phys 96:6325
50. Sok RM, Berendsen HJC, van Gunsteren WF (1992) J Chem Phys 96:4699
51. Kremer K, Grest G (1990) J Chem Phys 92:5057
52. McKechnie JI, Brown D, Clarke JHR (1992) Macromolecules 25:1562
53. Kotelyanskii MJ, Suter UW (1992) J Chem Phys 96:5383
54. McCoy JD, Honell KG, Curro JG, Schweizer KS, Honeycutt JD (1992) Macromolecules 25:4905
55. Khare R, Paulaitis ME, Lustig SR (1993) Macromolecules 26:7203
56. Dodd LR, Boone TD, Theodorou DN (1993) Mol Phys 78:961
57. Weiner SJ, Kollman PA, Case DA, Singh UC, Ghio C, Alagona G, Profeta Jr S, Weiner P (1984) J Am Chem Soc 106:765
58. Frisch MJ, Head-Gordon M, Trucks GW, Foresman JB, Schlegel HB, Raghavachari K, Robb M, Binkley JS, Gonzales C, Defrees DJ, Fox DJ, Whiteside RA, Seeger R, Melius CF, Baker J, Martin RL, Kahn RL, Stewart JJP, Topiol S, Pople JA, Gaussian 90, Gaussian Inc 6823 North Lakewood, Chicago, IL 60626

59. Batoulis J, Pittel B. (in preparation)
60. Rosenbluth M, Rosenbluth A (1955) J Chem Phys 23:356
61. Batoulis J, Kremer K (1988) J Phys A 21:127
62. Neumann KU, Schärpf O, Ziebeck KRA (1992) Physica B 180 & 181:817

Received April 25, 1994;
accepted June 16, 1994

Authors' address:

Prof. Dr. D. Richter
Institut für Festkörperforschung
Forschungszentrum Jülich
52425 Jülich, FRG.